

A RANGE CHARACTERIZATION OF THE SINGLE-QUADRANT ADRT

WEILIN LI*, KUI REN†, AND DONSUB RIM‡

Abstract. This work characterizes the range of the single-quadrant approximate discrete Radon transform (ADRT) of square images. The characterization follows from a set of linear constraints on the codomain. We show that for data satisfying these constraints, the exact and fast inversion formula [Rim, *Appl. Math. Lett.* **102** 106159, 2020] yields a square image in a stable manner. The range characterization is obtained by first showing that the ADRT is a bijection between images supported on infinite half-strips, then identifying the linear subspaces that stay finitely supported under the inversion formula.

Key words. approximate discrete Radon transform, range characterization, fast algorithms

AMS subject classifications. 44A12, 65R10, 92C55, 68U05, 15A04

1. Introduction. The Radon transform of functions defined on the Euclidean plane \mathbb{R}^2 is a transform that computes the integral of the function over all straight lines [31]. The lines are parametrized by two variables, so the transformed function is defined on the two dimensional (2D) cylinder $\mathbb{R} \times [-\pi, \pi]$. The Radon transform plays a fundamental role in many areas in both theoretical and applied mathematics. Perhaps the most widely known application is in the field of inverse problems, as a mathematical model of medical imaging techniques like computerized tomography (CT) [6, 27]. We will refer to the Radon transform as the *continuous* Radon transform, to distinguish it from its discretizations.

The range of continuous Radon transform, when it is applied to the class of smooth compactly supported functions on \mathbb{R}^2 , form a strict linear subspace of the codomain of smooth compactly supported functions on the cylinder [10]. Naturally, the inverse of the transform is well-defined only on the range, so it is important to be able to verify whether the given data to be inverted lies in the range. Range characterization refers to a precise description of this strict subspace. In most applications the data almost never lies in the range due to measurement noise, and in such situations the range characterization enables one to derive accurate and efficient methods for mapping the data back into the range so the inverse can be computed. These theoretical and practical issues have been studied carefully in the past, and we refer the reader to standard texts on the topic for general review [7, 10, 27].

*Courant Institute of Mathematical Sciences, New York University, New York, NY 10012 (weilinli@cims.nyu.edu)

†Department of Applied Physics and Applied Mathematics, Columbia University, New York, NY 10027 (kr2002@columbia.edu)

‡Department of Mathematics and Statistics, Washington University in St. Louis, St. Louis, MO 63105 (rim@wustl.edu)

There are many range characterization results for the continuous Radon transform and its generalizations. In fact, the singular value decomposition (SVD) of the transform is known in various settings [27, 24, 30, 22, 23, 15]. The decomposition is a fundamental tool for analyzing and building algorithms in situations where there are only finite or incomplete data [18, 19, 20, 21]. In case the function to be transformed is defined on the torus $\mathbb{T}^n = \mathbb{R}^n/\mathbb{Z}^n$ there are explicit results given in terms of the Fourier coefficients [11, 32], and for tensors on the slab $[0, 1] \times \mathbb{T}^n$ a non-trivial kernel can be characterized [14]. Furthermore, range characterizations in the Riemannian setting is currently an area of active research [13].

To perform practical computations, it is necessary to consider finite dimensional discretizations of the continuous Radon transform. Many of these discretizations were suitably devised for specific applications, but a general-purpose numerical discretization of the transform has only more recently attracted careful attention. Brief overviews of these methods appear in [28, 2]. These discretizations of the Radon transform also typically map a discretized 2D function onto a range that forms a strict subspace of the codomain, as in the continuous case. This work concerns the range characterization of a particular choice of discretization.

The Approximate Discrete Radon Transform (ADRT) is a fast multi-resolution algorithm that approximates the continuous Radon transform [5, 9]. The ADRT substitutes the integral over straight lines in the continuous Radon transform with a sum of point-values lying in the so-called digital lines. The ADRT for a 2D image is assembled from four identical single-quadrant ADRTs, performed on the properly rotated versions of the image.

The single-quadrant ADRT is a mapping from $N \times N$ square images with N^2 degrees of freedom to a larger codomain with $3N^2/2 - N/2$ degrees of freedom. In this work, we study this redundancy in the codomain and characterize the range of ADRT. We will specify precise constraints on the codomain that yields the range. We begin by considering the single-quadrant ADRT to be a map taking the space of images supported on an infinite half-strip into itself and then showing that it is a bijection in that setting, by the virtue of its exact inversion formula. Next we show that, for the original image to have been finitely supported, its ADRT must satisfy a set of linear constraints. We shall show that there are $N(N - 1)/2$ such linearly independent constraints, thereby prescribing the range that necessarily has N^2 degrees of freedom. The range characterization presented in this work is the first of its kind for any of the fast discretizations of the Radon transform, to the best of our knowledge.

It was the work of Press [28] that first demonstrated that the ADRT can be inverted to numerical precision by devising a multi-grid method. Press also conjectured the existence of an multi-grid variant of complexity $\mathcal{O}(N^2(\log N)^2 \log \varepsilon)$ for given error threshold $\varepsilon \in (0, 1)$. Subsequently, the single-quadrant ADRT was found to have

an exact and fast inverse of cost $\mathcal{O}(N^2 \log N)$ in [34]. This further revealed the ADRT to have a four-fold redundancy. The range characterization in this work is a consequence of this inverse, and it can be potentially useful in developing new projection techniques or iterative methods for inverting the ADRT.

Various other efficient discretizations of the Radon transform have been proposed [3, 16, 25, 36, 2, 1, 12], along with methods for computing their inverses. What sets ADRT apart is that it has an inversion formula that is both *fast* and *exact*; the inverse can be computed in $\mathcal{O}(N^2 \log N)$ operations, and in the absence of numerical error in the finite-precision operations, the formula would recover the original image exactly. Furthermore, this inverse for the single-quadrant ADRT is derived neither from the normal equations of the forward transform, nor the Fourier slice theorem [27]. Rather, it exploits a type of localization property, that the single-quadrant ADRT of a half-image can be computed from that of the full-image in $\mathcal{O}(N^2)$ operations. Despite enjoying these properties that the continuous Radon transform does not, the ADRT still converges to the continuous transform as $N \rightarrow \infty$ in the case the square image was formed by appropriately sampling a Lipschitz continuous image [5, 9].

The efficiency of both the forward and the inverse ADRT makes it suitable for use in applications. Besides from its well-known importance in tomography problems arising in medical imaging, radar imaging, geophysical imaging [7, 27] or electron microscopy [26, 8], it is also useful in computing generalizations of Lax-Philips representation [17, 4, 35, 33]. While the range characterization is the sole focus here, the characterization will be useful in these applications as well.

2. Digital lines and the ADRT. We will introduce notations and definitions, and recall the single-quadrant ADRT and its dual. Most of this section is a review of known definitions and properties [5, 9, 28].

We denote the set of integers as \mathbb{Z} and that of non-negative integers as \mathbb{N} . We will make use of a set of indices $I_m := \{i \in \mathbb{N} : i < m\}$ with $m \in \mathbb{N}$. Let us define the binary operator $\% : \mathbb{N} \times \mathbb{N} \rightarrow \mathbb{N}$ as the remainder $a \% b := a - \lfloor a/b \rfloor \cdot b$ for $a, b \in \mathbb{N}$.

We define the linear spaces of images defined on the vertical strip $\mathbb{Z} \times I_{2^n}$,

$$\begin{aligned} \mathcal{F}^n &:= \{f : \mathbb{Z} \times I_{2^n} \rightarrow \mathbb{R}\} && \text{(images on the vertical strip),} \\ \mathcal{F}_+^n &:= \{f \in \mathcal{F}^n : f(i, \cdot) \equiv 0 \text{ for } i \leq b_f, b_f \in \mathbb{Z}\} && \text{(images on the vertical half-strip),} \\ \mathcal{F}_0^n &:= \{f \in \mathcal{F}^n : \text{supp } f \subset I_{2^n} \times I_{2^n} < \infty\} && \text{(images on the square).} \end{aligned}$$

As the naming suggests, \mathcal{F}^n is the space of images defined on the vertical strip $\mathbb{Z} \times I_{2^n}$, \mathcal{F}_+^n contains images whose support is bounded below, that is, its support is contained in a vertical half-strip, and \mathcal{F}_0^n is the space of square images, as extended to the vertical strip. Needless to say, $\mathcal{F}_0^n \subset \mathcal{F}_+^n \subset \mathcal{F}^n$.

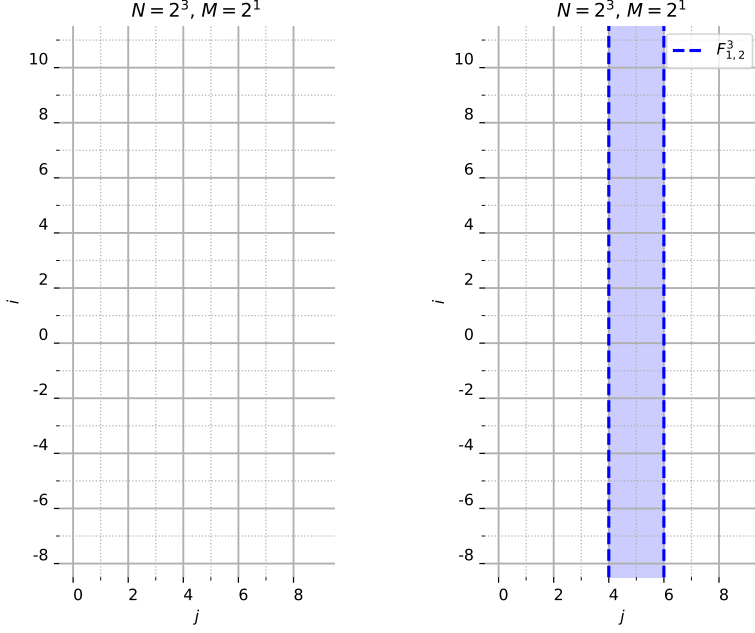


Fig. 2.1: A plot of the grid $\mathbb{Z} \times I_{2^n}$ and its indexing (left), and a plot highlighting the indices used for the section $f_{m,\ell}^n$ in Definition 2.1 (right) for the case $n = 3, m = 1, \ell = 2$.

The dot product for $f, g \in \mathcal{F}^n$ is given by $f \cdot g := \sum_{(i,j) \in \mathbb{Z} \times I_{2^n}} f(i,j)g(i,j)$. We will set the grid-size by $N := 2^n$ for some $n \in \mathbb{N}$.

A section is a restriction of image f to a vertical strip of width 2^m .

DEFINITION 2.1. *Given $f \in \mathcal{F}^n$, $m \in I_{n+1}$, $\ell \in I_{2^{n-m}}$, we define (m, ℓ) -section of f as $f_{m,\ell}^n \in \mathcal{F}^m$ taking on the values*

$$(2.1) \quad f_{m,\ell}^n(i, j) := f(i, j + \ell 2^m), \quad (i, j) \in \mathbb{Z} \times I_{2^m}.$$

For each $f \in \mathcal{F}^n$, the section $f_{m,\ell}^n$ merely accesses the entries that lie on the narrower vertical strip $\{(i, j + \ell 2^m) \mid (i, j) \in \mathbb{Z} \times I_{2^m}\}$. It is sometimes convenient to reverse the assignment (2.1),

$$(2.2) \quad f(i, j) = f_{m, \lfloor j/2^m \rfloor}^n(i, j \% 2^m), \quad (i, j) \in \mathbb{Z} \times I_{2^n}.$$

Throughout, we will adopt the convention that whenever the superscript and the first subscript agree, the subscripts are suppressed. For example, $f^n := f_n^n := f_{n,0}^n$.

The ADRT approximates the continuous Radon transform by substituting an integral over the straight lines in favor of a sum over the so-called digital lines, which we now define. A digital line is a recursively defined collection of points in $\mathbb{Z} \times I_{2^n}$.

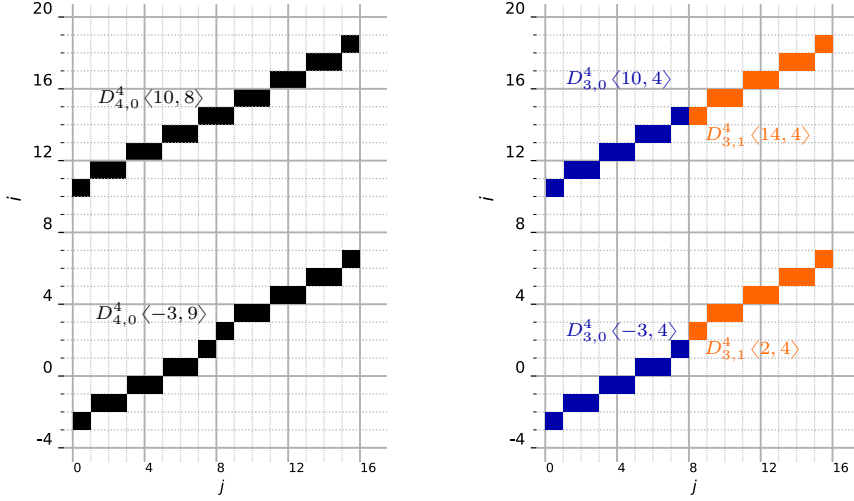


Fig. 2.2: A diagram depicting the recursive definition of a digital line (Definition 2.2).

DEFINITION 2.2. A digital line $D_{m,\ell}^n \langle h, s \rangle$ for $(h, s) \in \mathbb{Z} \times I_{2^m}$ is a subset of $\mathbb{Z} \times I_{2^n}$ that is defined recursively. Letting $s = 2t$ or $s = 2t + 1$,

$$(2.3) \quad \begin{cases} D_{m,\ell}^n \langle h, 2t + 1 \rangle := D_{m-1,2\ell}^n \langle h, t \rangle \cup D_{m-1,2\ell+1}^n \langle h + t + 1, t \rangle, \\ D_{m,\ell}^n \langle h, 2t \rangle := D_{m-1,2\ell}^n \langle h, t \rangle \cup D_{m-1,2\ell+1}^n \langle h + t, t \rangle, \end{cases}$$

and the relation is initialized by $D_{0,\ell}^n \langle h, \ell \rangle := \{(h, \ell)\}$ for $h \in \mathbb{Z}$, $\ell \in I_{2^n}$.

By its definition, the points of the digital line $D_{m,\ell}^n$ are contained in the narrow vertical strip $\mathbb{Z} \times \{s + \ell 2^m \mid s \in I_{2^m}\}$ of width 2^m . The digital line can also be defined to take as arguments $(h, s) \in \mathbb{Z} \times I_{2^n}$, that is

$$(2.4) \quad D_m^n \langle h, s \rangle := D_{m, \lfloor s/2^m \rfloor}^n \langle h, s \% 2^m \rangle, \quad (h, s) \in \mathbb{Z} \times I_{2^n},$$

in a similar manner as (2.2).

We define the single-quadrant ADRT as a summation of point values of f over the digital lines.

DEFINITION 2.3. Given the image $f \in \mathcal{F}^n$ and indices $m \in I_{n+1}$, $\ell \in I_{2^n-m}$, the (m, ℓ) -single-quadrant ADRT $R_{m,\ell}^n : \mathcal{F}^n \rightarrow \mathcal{F}^m$ is a linear operator given by

$$(2.5) \quad R_{m,\ell}^n[f](h, s) := \sum_{(i,j) \in D_{m,\ell}^n \langle h, s \rangle} f(i, j), \quad (h, s) \in \mathbb{Z} \times I_{2^m}.$$

We also define the m -single-quadrant ADRT by $R_m^n : \mathcal{F}^n \rightarrow \mathcal{F}^n$,

$$(2.6) \quad R_m^n[f](h, s) := R_{m, \lfloor s/2^m \rfloor}^n[f](h, s \% 2^m) = \sum_{(i,j) \in D_m^n \langle h, s \rangle} f(i, j), \quad (h, s) \in \mathbb{Z} \times I_{2^n}.$$

In particular, when $m = n$ we call the sum the single-quadrant ADRT of f , denoted by $R^n[f] := R_n^n[f] = R_{n,0}^n[f]$.

The two definitions $R_{m,\ell}^n[f]$ and $R_m^n[f]$ are two different ways of indexing an identical set of values: If $g = R_m^n[f] \in \mathcal{F}^n$ then its section $g_{m,\ell}^n = R_{m,\ell}^n[f] \in \mathcal{F}^m$. Going forward, we will use the indices $(i, j) \in \mathbb{Z} \times I_{2^n}$ when referencing the individual values of an image f , and indices $(h, s) \in \mathbb{Z} \times I_{2^n}$ when referencing digital lines $D_{m,\ell}^n \langle h, s \rangle$ or the ADRT $R_{m,\ell}^n[f](h, s)$. The notation (h, s) is due to Press [28]; h stands for height and s for slope, respectively.

Observe that for R_m^n the codomain is equal to the domain, both \mathcal{F}^n . This corresponds to how the continuous Radon transform maps the vertical strip $\mathbb{R} \times [0, 1]$ into $\mathbb{R} \times [0, \pi]$ (see [27]) except that the single-quadrant ADRT only concerns a quarter of the angles $[0, \pi/4]$ rather than $[0, \pi]$.

Due to the recursive definition of the digital lines in Definition 2.2, the summation (2.5) can also be computed recursively. Let us define the linear operator $S_m : \mathcal{F}^{m-1} \times \mathcal{F}^{m-1} \rightarrow \mathcal{F}^m$ by

$$(2.7) \quad \begin{cases} S_m[f_0, f_1](h, 2t) = f_0(h, t) + f_1(h + t, t), \\ S_m[f_0, f_1](h, 2t + 1) = f_0(h, t) + f_1(h + t + 1, t). \end{cases}$$

The same operation can be defined on \mathcal{F}^n : Let us define $S_m^n : \mathcal{F}^n \rightarrow \mathcal{F}^n$ as given by

$$(2.8) \quad S_m^n[f] := g, \quad \text{where } g_{m,\ell'}^n = S_m[f_{m-1,2\ell'}^n, f_{m-1,2\ell'+1}^n] \text{ for } \ell' \in I_{2^{n-m-1}}.$$

The operator S_m^n merely applies S_m to the pairs of the individual sections of an image in \mathcal{F}^n , so it is well-defined and linear. Put another way, the operation by S_m^n can be broken down into four smaller steps:

- (i) Take an image in $f \in \mathcal{F}^n$ and extract its $(m-1, \ell)$ -sections $f_{m-1,\ell}^n \in \mathcal{F}^{m-1}$,
- (ii) pair the sections $(f_{m-1,2\ell'}^n, f_{m-1,2\ell'+1}^n) \in \mathcal{F}^{m-1} \times \mathcal{F}^{m-1}$ where $\ell' \in I_{2^{n-m-1}}$,
- (iii) apply S_m to these 2^{n-m-1} pairs and obtain images in \mathcal{F}^m ,
- (iv) create a new image $g \in \mathcal{F}^n$ by defining its (m, ℓ') -sections \mathcal{F}^m as the images in \mathcal{F}^m obtained in the previous step.

Then $R_m^n[f]$ is equal to a sequential application of S_m^n

$$(2.9) \quad R_m^n[f] = S_m^n \circ S_{m-1}^n \circ \cdots \circ S_1^n[f_{m,\ell}^n], \quad m \in I_{n+1}.$$

If $f \in \mathcal{F}_0^n$, then a single application of S_m^n has the computational complexity $\mathcal{O}(N^2)$, thus $R_m^n[f]$ costs $\mathcal{O}(N^2 \log N)$.

2.1. Dual digital lines and back-projection. We will next describe the dual digital lines and the back-projection. An interesting feature of the dual of digital lines satisfy a similar recursive property; they are almost themselves digital lines, save that

they have negative slopes.

DEFINITION 2.4. A dual digital line $D'_{m,\ell} \langle i, j \rangle$ for $(i, j) \in \mathbb{Z} \times I_{2^m}$ is defined as

$$(2.10) \quad D'_{m,\ell} \langle i, j \rangle := \{(h, s) \in \mathbb{Z} \times I_{2^n} \mid (i, j + \ell 2^m) \cap D_m^n \langle h, s \rangle \neq \emptyset\}.$$

The dual digital lines $D'_{m,\ell}$ are defined as the collection of digital lines that pass through the point $(i, j + \ell 2^m) \in \mathbb{Z} \times I_{2^n}$. Since digital lines D_m^n are indexed by $(h, s) \in \mathbb{Z} \times I_{2^n}$, this collection of digital lines can be identified to a collection of points in $\mathbb{Z} \times I_{2^n}$. In this sense, the dual digital lines $D'_{m,\ell}$ also form a collection of these points, like the digital lines. See Figure 2.3 for an example. Furthermore, as was done for $D'_{m,\ell}$, we let

$$(2.11) \quad D_m^n \langle i, j \rangle := D'_{m, \lfloor j/2^m \rfloor} \langle i, j \% 2^m \rangle, \quad (i, j) \in \mathbb{Z} \times I_{2^n}.$$

Now, just as the sum over the digital lines define the ADRT R_m^n , the sum over the dual digital lines define the back-projection of the single-quadrant ADRT.

DEFINITION 2.5. We define the (m, ℓ) -back-projection as $R'_{m,\ell} : \mathcal{F}^n \rightarrow \mathcal{F}^m$ as a linear operator given by

$$(2.12) \quad R'_{m,\ell}[g](i, j) := \sum_{(h,s) \in D'_{m,\ell} \langle i, j \rangle} g(h, s), \quad (i, j) \in \mathbb{Z} \times I_{2^m},$$

and we will also define the m -back-projection $R_m^n : \mathcal{F}^n \rightarrow \mathcal{F}^n$ by

$$(2.13) \quad R_m^n[g](i, j) := R'_{m, \lfloor j/2^m \rfloor}[g](h, j \% 2^m) = \sum_{(h,s) \in D_m^n \langle i, j \rangle} g(h, s), \quad (i, j) \in \mathbb{Z} \times I_{2^n}.$$

Let $\delta_{i,j}^m$ denote the Kronecker delta. For $m \in \mathbb{N}$, $(i, j), (i', j') \in \mathbb{Z} \times I_{2^n}$, let $\delta_{i,j}^m \in \mathcal{F}^m$ be given by $\delta_{i,j}^m(i', j') = 1$ if $(i, j) = (i', j')$ and $\delta_{i,j}^m(i', j') = 0$ otherwise.

The digital line D_m^n and its dual $D'_{m,\ell}$ can be expressed in terms of R_m^n and $R'_{m,\ell}$, respectively.

LEMMA 2.6. The digital line D and its dual D' are related by

$$(2.14) \quad \chi_{D'_{m,\ell} \langle i, j \rangle} = R_m^n[\delta_{i,j}^n], \quad \chi_{D_m^n \langle h, s \rangle} = R'_{m,\ell}[\delta_{h,s}^n].$$

Proof. Since $(i, j) \in D'_{m,\ell} \langle h, s \rangle$ if and only if $(h, s) \in D_m^n \langle i, j \rangle$,

$$(2.15) \quad R'_{m,\ell}[\delta_{i,j}^n](h, s) = \chi_{D_m^n \langle h, s \rangle}(i, j) = \chi_{D'_{m,\ell} \langle i, j \rangle}(h, s) = R_m^n[\delta_{h,s}^n](i, j). \quad \square$$

Therefore, one can also express the digital line $D'_{m,\ell}$ and its dual D_m^n in terms

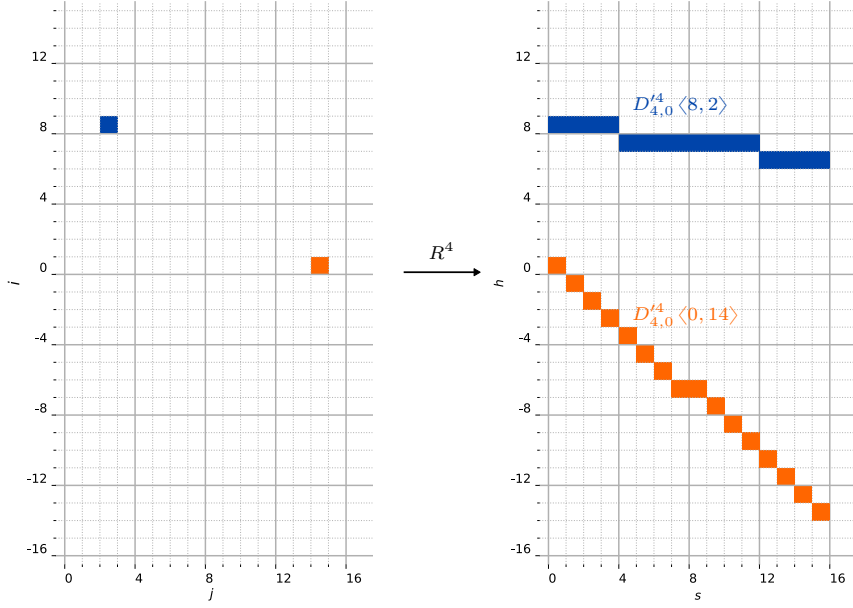


Fig. 2.3: Diagram depicting a dual digital line [Definition 2.2](#).

of the back-projection $R_m'^n$ and the single-quadrant ADRT R_m^n ,

$$(2.16) \quad D_{m,\ell}^n \langle h, s \rangle = \text{supp } R_m'^n[\delta_{h,s}^n], \quad D_{m,\ell}^n \langle i, j \rangle = \text{supp } R_m^n[\delta_{i,j}^n].$$

With these observations at hand, it is straightforward to show that R'^n is the transpose of R^n .

LEMMA 2.7. R'^n is the transpose of R^n .

Proof. From the definitions,

$$(2.17) \quad \begin{aligned} (h, s) \in D'^n \langle i, j \rangle &\Leftrightarrow \delta_{h,s}^n \cdot \chi_{D'^n \langle i, j \rangle} = 1 \\ &\Leftrightarrow (i, j) \in D^n \langle h, s \rangle \Leftrightarrow \delta_{i,j}^n \cdot \chi_{D^n \langle h, s \rangle} = 1. \end{aligned}$$

Then directly,

$$(2.18) \quad \delta_{h,s}^n \cdot R^n[\delta_{i,j}^n] = \delta_{h,s}^n \cdot \chi_{D'^n \langle i, j \rangle} = \chi_{D^n \langle h, s \rangle} \cdot \delta_{i,j}^n = \delta_{i,j}^n \cdot R'^n[\delta_{h,s}^n]. \quad \square$$

In the same manner in which R_m^n was expressed as a composition of a sequence of S_m^n , the transpose $R_m'^n$ also attains an expression as compositions. Define the linear operator $B_m : \mathcal{F}^{m+1} \rightarrow \mathcal{F}^m \times \mathcal{F}^m$ which reverses the addition of S_m^n (2.7): we sum the terms of g that contribute to $g_0(h, t)$ which are $g(h, 2t+1)$ and $g(h, 2t)$, and those

that contribute to $g_1(h, t)$, which are $g(h - t - 1, 2t + 1)$ and $g(h - t, 2t)$. That is,

$$(2.19) \quad B_m[g] := [g_0, g_1], \quad \begin{cases} g_0(h, t) := g(h, 2t) + g(h, 2t + 1), \\ g_1(h, t) := g(h - t, 2t) + g(h - t - 1, 2t + 1). \end{cases}$$

We define an identical operation $B_m^n : \mathcal{F}^n \rightarrow \mathcal{F}^n$ over larger images by

$$(2.20) \quad B_m^n[f] := g, \quad [g_{m-1, 2\ell'}, g_{m-1, 2\ell'+1}] = B_m[f_{m, \ell'}], \quad \ell' \in I_{2^{n-m-1}}.$$

It follows that $R_{m, \ell}'^n$ is a repeated application of B_m^n ,

$$(2.21) \quad R_m^n[g] = B_1^n \circ \cdots \circ B_m^n[g], \quad \text{for } m \in I_{n+1}.$$

Naturally, the dual digital line D' satisfies a recursive relation that is very similar to that of D .

COROLLARY 2.8. *A dual digital line $D_{m, \ell}'^n \langle h, s \rangle$ for $(h, s) \in \mathbb{Z} \times I_{2^m}$ is a subset of $\mathbb{Z} \times I_{2^n}$ that satisfies*

$$(2.22) \quad \begin{cases} D_{m, \ell}'^n \langle h, 2t \rangle := D_{m-1, 2\ell}'^n \langle h, t \rangle \cup D_{m-1, 2\ell+1}'^n \langle h - t, t \rangle, \\ D_{m, \ell}'^n \langle h, 2t + 1 \rangle := D_{m-1, 2\ell}'^n \langle h, t \rangle \cup D_{m-1, 2\ell+1}'^n \langle h - t - 1, t \rangle, \end{cases}$$

and the relation is initialized by $D_{0, \ell}'^n \langle h, \ell \rangle := \{(h, \ell)\}$, for $h \in \mathbb{Z}$, $\ell \in I_{2^n}$.

One may derive direct formulas for the digital lines and their duals, without the use of a recursion. Perhaps not so efficient to use for computation, they reveal that the two definitions they are identical up to the sign of its increments.

COROLLARY 2.9. *Let $(s)_2$ denote the binary representation of $s \in \mathbb{N}$, \wedge the bit-wise and, \neg the bit-wise not, $*$ the bitwise inner product, and $\overline{(s)}_2$ the bit reversal of $(s)_2$.*

(i) $D_m^n \langle h, s \rangle = \{(k_+(t), t) \in \mathbb{Z} \times I_{2^n}\}$ in which $k_+ : I_N \rightarrow \mathbb{Z}$ satisfies

$$(2.23) \quad \begin{cases} k_+(t) - k_+(t-1) = ((t)_2 \wedge \neg(t-1)_2) * \overline{(s)}_2, \\ k_+(0) = h. \end{cases}$$

(ii) $D_m^n \langle h, s \rangle = \{(k_-(t), t) \in \mathbb{Z} \times I_N\}$ in which $k_- : I_N \rightarrow \mathbb{Z}$ satisfies

$$(2.24) \quad \begin{cases} k_-(t-1) - k_-(t) = ((t)_2 \wedge \neg(t-1)_2) * \overline{(s)}_2, \\ k_-(0) = h. \end{cases}$$

The increments in (2.23) for a sequence of digital lines, for whom the ratio $s/(N-1)$ is constant, is shown in subsection 2.1. The distribution of the increments is reminiscent of the low-discrepancy sequences [29].

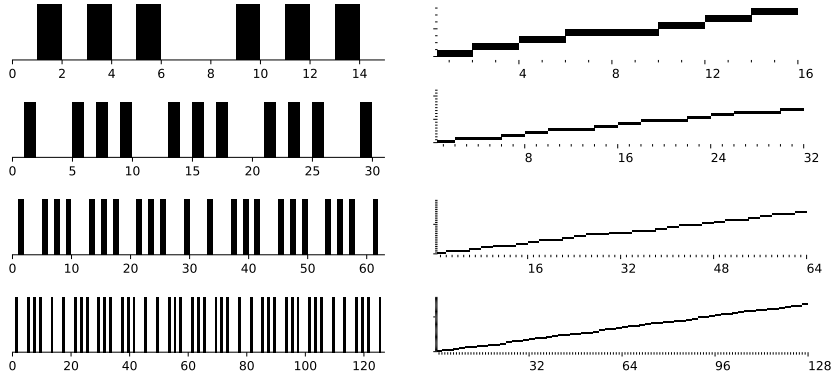


Fig. 2.4: Diagram depicting the increments (left) of corresponding digital lines (right).

2.2. Exact inverse. An important property of the single-quadrant ADRT is that it has an exact and fast inversion formula.

THEOREM 2.10 (Rim [34]). *If $f \in \mathcal{F}_0^n$ then $R_{m-1,2\ell}^n[f]$ and $R_{m-1,2\ell+1}^n[f]$ can be computed from $R_{m,\ell}^n[f]$ for all $m \in I_{n+1}, \ell \in I_{2^{n-m}}$ in $\mathcal{O}(N^2)$ operations.*

We will briefly review the inversion formula. Let us define the differences,

$$(2.25) \quad \Delta_{m,\ell}^n[f](h, s) := R_{m,\ell}^n[f](h+1, s) - R_{m,\ell}^n[f](h, s),$$

then these differences can be computed by the relations, for all $\ell' \in I_{2^{n-m-1}}$

$$(2.26) \quad \Delta_{m-1,2\ell'}^n[f](h, s) = R_{m,\ell'}^n[f](h+1, 2s) - R_{m,\ell'}^n[f](h, 2s+1),$$

$$(2.27) \quad \Delta_{m-1,2\ell'+1}^n[f](h, s) = R_{m,\ell'}^n[f](h-s, 2s+1) - R_{m,\ell'}^n[f](h-s, 2s).$$

Using the differences, one recovers the $(m-1, \ell)$ -single-quadrant ADRT,

$$(2.28) \quad R_{m-1,\ell}^\ell[f](h, s) = \sum_{k=-s}^{h-1} \Delta_{m-1,\ell}^n[f](k, s).$$

So we obtain the formulae for $\ell' \in I_{2^{n-m-1}}$,

$$(2.29) \quad \begin{aligned} R_{m-1,2\ell'}^n[f](h, s) &= \sum_{k=-s}^{h-1} [R_{m,\ell'}^n[f](k+1, 2s) - R_{m,\ell'}^n[f](k, 2s+1)], \\ R_{m-1,2\ell'+1}^n[f](h, s) &= \sum_{k=-s}^{h-1} [R_{m,\ell'}^n[f](k-s, 2s+1) - R_{m,\ell'}^n[f](k-s, 2s)], \end{aligned}$$

which yields the theorem.

This formula is readily extended to apply to images in \mathcal{F}_+^n . Then, the operation given by this formula is the inverse of $S_m : \mathcal{F}_+^n \rightarrow \mathcal{F}_+^n$. Let us use a notation for the operation (2.29), say $S_m^{-1} : \mathcal{F}_+^m \rightarrow \mathcal{F}_+^{m-1} \times \mathcal{F}_+^{m-1}$. That is, for $g \in \mathcal{F}_+^m$,

$$(2.30) \quad S_m^{-1}[g] := [g_0, g_1],$$

$$\begin{cases} g_0(h, s) = \sum_{k=-\infty}^{h-1} [g(k+1, 2s) - g(k, 2s+1)], \\ g_1(h, s) = \sum_{k=-\infty}^{h-1} [g(k-s, 2s+1) - g(k-s, 2s)], \end{cases}$$

then the inversion formula (2.29) can be written as

$$(2.31) \quad S_m^{-1}[R_{m,\ell'}^n[f]] = [R_{m-1,2\ell'}^n[f], R_{m-1,2\ell'+1}^n[f]].$$

Let $(S_m^n)^{-1} : \mathcal{F}_+^n \rightarrow \mathcal{F}_+^n$ be defined

$$(2.32) \quad (S_m^n)^{-1}[g] := f \quad \text{with} \quad [f_{m-1,2\ell'}^n, f_{m-1,2\ell'+1}^n] = S_m^{-1}[f_{m,\ell'}^n], \quad \ell \in I_{2^n-m}.$$

Then we have

$$(2.33) \quad (R_m^n)^{-1}[g] = (S_1^n)^{-1} \circ \dots \circ (S_m^n)^{-1}[g].$$

COROLLARY 2.11. *The inverse of single-quadrant ADRT $(R^n)^{-1} : R^n[\mathcal{F}_0^n] \rightarrow \mathcal{F}_0^n$ is given by*

$$(2.34) \quad (R^n)^{-1}[g] = (S_1^n)^{-1} \circ \dots \circ (S_n^n)^{-1}[g].$$

Thus, the computational complexity of computing R^n is equal to that of computing $(R^n)^{-1}$, both $\mathcal{O}(N^2 \log N)$.

The direction of the sum in (2.30) is not a unique choice. If so inclined, one may sum from $+\infty$ to h , granted the original image f is taken from the half-vertical strip that is unbounded in the negative i -direction, say \mathcal{F}_-^n . In the case $f \in \mathcal{F}_0$, one may also take an average of two sums ranging from $-\infty$ to ∞ . We will continue with one-sided sum here, and in section 3, it will become clear that this choice coincides with a back-substitution formula.

3. Range characterization. This section contains the range characterization of the single-quadrant ADRT over square images \mathcal{F}_0^n . We proceed by first showing that $R^n : \mathcal{F}_+^n \rightarrow \mathcal{F}_+^n$ is a bijection, due to the exact inversion formula. Next, we find $\mathcal{F}_R^n \subset \mathcal{F}_+^n$ for which $R^n : \mathcal{F}_0^n \rightarrow \mathcal{F}_R^n$ is a bijection, thereby characterizing the range of R^n over square images.

3.1. Characterization of $R^n[\mathcal{F}_+^n]$. The inversion formula (2.29) leads to the fact that R^n is bijective. This is summed up in a corollary.

COROLLARY 3.1. $R^n(R^n)^{-1}[\delta_{h,s}^n] = \delta_{h,s}^n$ and $(R^n)^{-1}R^n[\delta_{i,j}^n] = \delta_{i,j}^n$.

Proof. By the virtue of (2.31), $(S_k) \circ (S_k)^{-1}[\delta_{h,s}^{n-k+1}] = \delta_{h,s}^{n-k+1}$, so that

$$R^n(R^n)^{-1}[\delta_{h,s}^n] = (S_n^n) \circ \dots \circ (S_1^n) \circ (S_1^n)^{-1} \circ \dots \circ (S_n^n)^{-1}[\delta_{h,s}^n] = \delta_{h,s}^n.$$

Similarly, the latter identity follows from

$$\begin{aligned} (S_k)^{-1} \circ (S_k) \left[\delta_{h,s}^{n-k+1}, 0 \right] &= \left[\delta_{h,s}^{n-k+1}, 0 \right], \\ (S_k)^{-1} \circ (S_k) \left[0, \delta_{h,s}^{n-k+1} \right] &= \left[0, \delta_{h,s}^{n-k+1} \right], \end{aligned}$$

which can be verified from direct computation, for example,

$$\begin{aligned} (S_k)^{-1} \circ (S_k) \left[\delta_{h,s}^{n-k+1}, 0 \right] &= (S_k)^{-1} \left[\delta_{h,2s}^{n-k+2} + \delta_{h,2s+1}^{n-k+2} \right] \\ &= \left[\sum_{k=-\infty}^{h'-1} \delta_{h,s}^{n-k+1}(k+1, s') - \sum_{k=-\infty}^{h'-1} \delta_{h,s}^{n-k+1}(k, s'), 0 \right] \\ &= \left[\delta_{h,s}^{n-k+1}(h', s'), 0 \right], \end{aligned}$$

and the second equality follows similarly. \square

Furthermore, we will show that $R^n[\mathcal{F}_+^n] = \mathcal{F}_+^n$ by providing an explicit expression for $(R^n)^{-1}[\delta_{h,s}^n]$ for each $(h, s) \in \mathbb{Z} \times I_{2^n}$. First, it will be expedient to define the mapping $\lambda : \mathbb{Z} \times \mathbb{N} \times \{\pm 1\} \rightarrow (\mathbb{Z} \times \mathbb{N} \times \{\pm 1\})^2$

$$(3.1) \quad \lambda(h, s, \sigma) := [\lambda_0, \lambda_1], \quad \begin{cases} \lambda_0 := [h + (s \% 2), & [s/2], & \sigma \cdot (-1)^{(s \% 2)}], \\ \lambda_1 := [h + [s/2] + 1, & [s/2], & \sigma \cdot (-1)^{(s \% 2) + 1}]. \end{cases}$$

It is straightforward to show that λ is an injective map, as the pair $[\lambda_0, \lambda_1]$ uniquely defines the triple (h, s, σ) for which $\lambda(h, s, \sigma) = [\lambda_0, \lambda_1]$: denoting the three entries by $\lambda_0 = [\lambda_{0,0}, \lambda_{0,1}, \lambda_{0,2}]$, $\lambda_1 = [\lambda_{1,0}, \lambda_{1,1}, \lambda_{1,2}]$ one recovers e.g. $h = \lambda_{1,0} - \lambda_{1,1} - 1$, $s = \lambda_{0,0} + 2\lambda_{1,0} - 3h - 2$, $\sigma = \lambda_{0,2} \cdot (-1)^{(s \% 2)}$ successively.

Below, let $(\cdot)_+^i : \mathbb{R} \rightarrow \mathbb{R}_+$ is given by $(x)_+^i := \max\{0, x^i\}$ for $i \in \mathbb{N}$. When $i = 1$ it is also called the rectified linear unit (ReLU), and when $i = 0$ it is the Heaviside step function.

LEMMA 3.2. Let $(h, s, \sigma) \in \mathbb{Z} \times I_{2^m} \times \{\pm 1\}$ and let

$$(3.2) \quad \lambda_0 = [h_0, s_0, \sigma_0], \quad \lambda_1 = [h_1, s_1, \sigma_1], \quad \text{where } [\lambda_0, \lambda_1] = \lambda[h, s, \sigma].$$

Then $g_0, g_1 \in \mathcal{F}_+^m$ of the inverse $(S_m)^{-1}[\sigma \delta_{h,s}^m] = [g_0, g_1]$ are given by the formula

$$(3.3) \quad g_b(h, s) = \sigma_b \sum_{h' \geq h_b} \delta_{h', s_b}^{m-1}(h, s) = \sigma_b \delta_{s_b}^{m-1}(s)(h - h_b)_+^0, \quad b \in \{0, 1\}.$$

Proof. In the case s is even, let $s = 2t$ then

$$(3.4) \quad \begin{cases} g_0(h', s') = \sum_{k=-s'}^{h'-1} \delta_{h,s}^{m-1}(k+1, 2s') = \delta_t(s')(h' - h)_+^0, \\ g_1(h', s') = - \sum_{k=-s'}^{h'-1} \delta_{h,s}^{m-1}(k+1, 2s') = -\delta_t(s')(h' - h - t - 1)_+^0 \end{cases}$$

In case s is odd, let $s = 2t + 1$,

$$(3.5) \quad \begin{cases} g_0(h', s') = - \sum_{k=-s'}^{h'-1} \delta_{h,s}^{m-1}(k, 2s'+1) = -\delta_t(s')(h' - h - 1)_+^0, \\ g_1(h', s') = - \sum_{k=-s'}^{h'-1} \delta_{h,s}^{m-1}(k - s', 2s') = \delta_t(s')(h' - h - t - 1)_+^0. \end{cases}$$

These direct results are summarized via (3.1) and (3.3). \square

Observe that $\text{supp } S_m^{-1}[\delta_{h,s}^m]$ is unbounded in the positive h -direction and so belongs to \mathcal{F}_+^n . The vertical half-lines on which the inverse is supported is denoted by,

$$(3.6) \quad L^m(h, s) := \{(h', s') \in \mathbb{Z} \times I_{2^m} : h' \geq h, s' = s\},$$

so we can also write $(S_m)^{-1}[\sigma \cdot \delta_{h,s}^m] = [\sigma_0 \cdot \chi_{L^{m-1}(h_0, s_0)}, \sigma_1 \cdot \chi_{L^{m-1}(h_1, s_1)}]$.

A plot of the inverse $(S_n^n)^{-1}[\delta_{h,s}^n]$ is shown in Figure 3.1: the inverted image consists of two slices of vertically oriented jumps.

Then Lemma 3.2 and the decomposition of R^n (2.34) enable us to compute $(R^n)^{-1}[\delta_{h,s}^n]$. A repeated application of λ (3.1) yields,

$$(3.7) \quad \begin{aligned} \lambda_0 &= (h_0, s_0, \sigma_0), \quad \dots, \quad \lambda_{2^n-1} = (h_{2^n-1}, s_{2^n-1}, \sigma_{2^n-1}), \\ (\lambda_0, \dots, \lambda_{2^n-1}) &:= \underbrace{\lambda \otimes \dots \otimes \lambda}_{n \text{ times}}(h, s). \end{aligned}$$

For $t \in I_{2^m}$, we may rewrite λ_t in terms of the binary expansion $t = (b_0 b_1 \dots b_k)_2$ by the shorthand $\lambda_t = \lambda_{b_0 b_1 \dots b_k}$. Using this, one expresses diagrammatically the repeated application of the map λ (3.1),

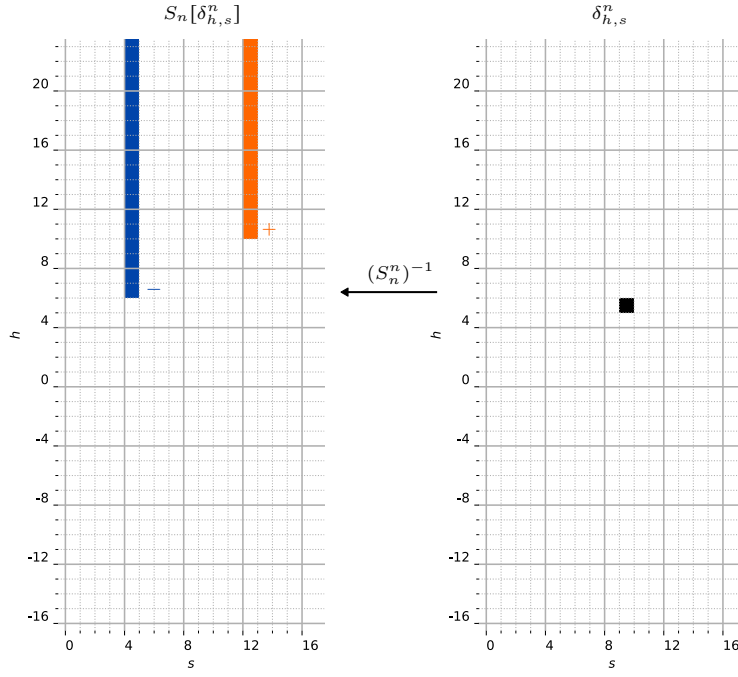
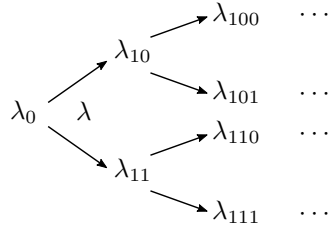


Fig. 3.1: A plot of $(S_n^n)^{-1}[\delta_{h,s}^n]$ given by the formula (2.31).



The indices $\{h_t\}_{t=0}^{2^n-1}$ then provide the lower bounds of the support of $(R^n)^{-1}[\delta_{h,s}^n]$. A little more precisely, the support equals the union of vertical half-lines

$$(3.8) \quad L_m^n(h, s) := \bigcup_{t \in I_{2^n-m}} L^n(h_t, s_t).$$

THEOREM 3.3. R^n is a bijection from \mathcal{F}_+^n onto itself. In particular, for each triple $(h, s, \sigma) \in \mathbb{Z} \times I_{2^n} \times \{\pm 1\}$,

$$(3.9) \quad (R^n)^{-1}[\sigma \delta_{h,s}^n](i, j) = \sigma_j (i - h_j)_+^{n-1}, \quad (i, j) \in \mathbb{Z} \times I_{2^n},$$

in which $(h_j, \sigma_j) \in \mathbb{Z} \times \{\pm 1\}$ as given in (3.7).

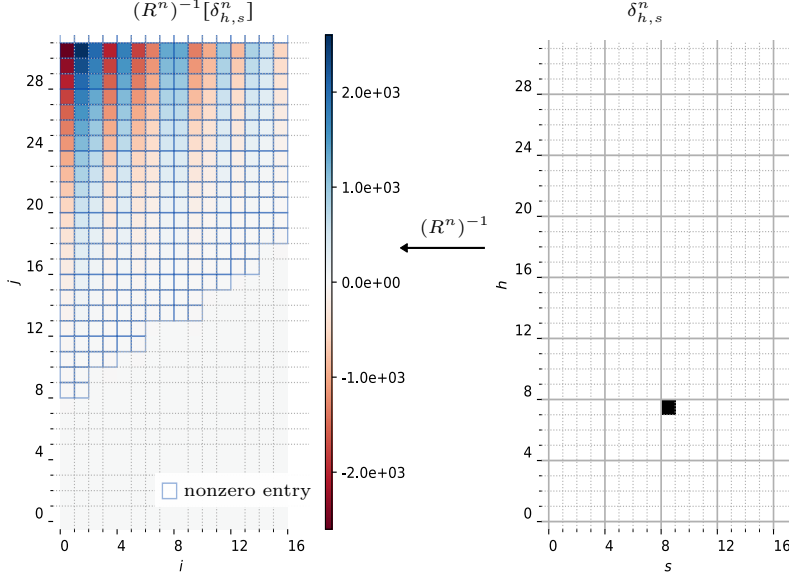


Fig. 3.2: A plot of $(R^n)^{-1}[\delta_{h,s}^n]$ given by the formula (3.9).

Proof. This follows from a repeated application of Lemma 3.2. Let us denote

$$\begin{aligned}
 (S_n)^{-1}[\delta_{h,s}^n] &= [g_0, g_1], \\
 (S_{n-1})^{-1}[g_0] &= [g_{00}, g_{01}], \quad (S_{n-1})^{-1}[g_1] = [g_{10}, g_{11}], \\
 &\vdots
 \end{aligned}
 \tag{3.10}$$

so that we can denote g_s using the binary expansion $s = (b_0 \cdots b_k)_2$ as follows,

$$(S_{n-k})^{-1}[g_{b_0 \cdots b_k}] = (g_{b_0 \cdots b_k b_{k+1}}, g_{b_0 \cdots b_k b_{k+1}}) \quad b_k \in \{0, 1\}.
 \tag{3.11}$$

We proceed by induction. Suppose that it holds

$$\begin{aligned}
 g_{b_0 \cdots b_k}(h', s') &= \sigma_{b_0 \cdots b_k} \delta_{s_{b_0 \cdots b_k}}^{n-k-1}(s')(h' - h_{b_0 \cdots b_k})_+^{k-1} \\
 &= \sigma_{b_0 \cdots b_k} \sum_{h \geq h_{b_0 \cdots b_k}} \delta_{h, s_{b_0 \cdots b_k}}^{n-k-1}(h', s')(h' - h_{b_0 \cdots b_k})_+^{k-1}.
 \end{aligned}
 \tag{3.12}$$

Then,

$$\begin{aligned}
 &(S_{n-k})^{-1}[g_{b_0 \cdots b_k}](h', s') \\
 &= (S_{n-k})^{-1} \left[\sigma_{b_0 \cdots b_k} \sum_{h \geq h_{b_0 \cdots b_k}} \delta_{h, s_{b_0 \cdots b_k}}^{n-k-1}(h', s')(h' - h_{b_0 \cdots b_k})_+^{k-1} \right] \\
 &= \sum_{j=1}^{\infty} (j)^{k-1} (S_{n-k+1})^{-1} \left[\sigma_{b_0 \cdots b_k} \delta_{h_{b_0 \cdots b_k} + j - 1, s_{b_0 \cdots b_k}}^{n-1}(h', s') \right]
 \end{aligned}
 \tag{3.13}$$

So it follows,

$$\begin{aligned}
(3.14) \quad g_{b_0 \dots b_{k+1}}(h', s') &= \sum_{j=1}^{\infty} (j)^{k-1} \sigma_{b_0 \dots b_{k+1}} \sum_{j'=1}^{\infty} \delta_{h_{b_0 \dots b_{k+1}} + j - 1 + j' - 1, s_{b_0 \dots b_{k+1}}}^{n-1}(h', s') \\
&= \sigma_{b_0 \dots b_{k+1}} \sum_{j=1}^{\infty} (j^{k-1} \cdot j) \delta_{h_{b_0 \dots b_{k+1}} + j - 1, s_{b_0 \dots b_{k+1}}}^{n-1}(h', s') \\
&= \sigma_{b_0 \dots b_{k+1}} \sum_{h \geq h_{b_0 \dots b_{k+1}}} \delta_{h, s_{b_0 \dots b_{k+1}}}^{n-1}(h', s') (h - h_{b_0 \dots b_{k+1}})_+^k.
\end{aligned}$$

Now, the case $k = 0$ follows by (3.3), proving the formula.

Since the map λ is injective, the formula (3.9) shows that $(R^n)^{-1}$ is injective. Thus R^n is a bijection. \square

It is worth noting that the continuous Radon transform does not possess an analogous property. The continuous inverse is ill-defined when applied to arbitrary functions in the unconstrained codomain [27]. In contrast, one can extend the inverse ADRT $(R^n)^{-1}$ from $R^n[\mathcal{F}_0^n]$ to the codomain \mathcal{F}_+^n , simply by enlarging the domain to allow infinitely supported images, that is, by extending R^n from \mathcal{F}_0^n to \mathcal{F}_+^n . Accordingly, this property of ADRT is unlikely to be preserved in the continuous limit.

The inverse image $(R^n)^{-1}[\delta_{h,s}^n]$ is plotted in Figure 3.1. One observes an oscillatory behavior in the i -direction, and a polynomial growth in the j -direction. The oscillation can be related to the oscillatory behavior of the non-unique solutions to the limited angle problem for the continuous Radon transform [27, Ch3]; the details of this relation will be pursued elsewhere.

Finally, we give a more explicit expression for the function λ .

COROLLARY 3.4. *Letting $s^{(k)} := \lfloor s/2^k \rfloor$, $s_r^{(k)} := (s^{(k-1)} \% 2)$, if $t \in I_{2^n}$ has the binary representation $t = (b_1 b_2 \dots b_n)_2$, then h_t, σ_t above in (3.7) can be written as*

$$(3.15) \quad h_t = h + \sum_{k=1}^n (b_k s^{(k)} + (1 - b_k) s_r^{(k)}), \quad \sigma_t = (-1)^{\varsigma_2(t \underline{\vee} s)},$$

where ς_2 is the bit-wise sum, and $\underline{\vee}$ is the bit-wise xor.

3.2. Conditional convergence for finitely supported images. The fact that R^n is a bijection from \mathcal{F}_+^n onto itself is dependent on the unboundedness of $\text{supp } f$ for $f \in \mathcal{F}_+^n$. The following observation shows that for R^n to be bijective the sums (2.29) appearing in the inversion formula must converge conditionally, as the summands exhibit polynomial growth. Moreover, the degree of the polynomial growth depends on n , and hence the inverse diverges as $N \rightarrow \infty$.

Let $\chi_k := \chi_{I_{(k+1)2^n} \times I_{2^n}}$ with $k \in \mathbb{N}$ denote the cut-off function supported in a

rectangle of width 2^n . Then,

$$\|R^n \chi_k (R^n)^{-1} - \text{Id}\|_\infty \gtrsim k^n \quad k \geq 1,$$

where $\|\cdot\|_\infty$ denotes for $B : \mathcal{F}_+^n \rightarrow \mathcal{F}_+^n$ the induced norm $\|B\|_\infty := \sup_{f \in \mathcal{F}_+^n} \frac{\|Bf\|_\infty}{\|f\|_\infty}$ with $\|f\|_\infty := \sup_{(h,s) \in \mathbb{Z} \times I_{2^n}} |f(h,s)|$.

This can be seen as follows. Choose $\delta_{h,s}^n$ with $(h,s) = (-2^n + 1, 2^n - 1)$, and let $[h_{2^n-1}, s_{2^n-1}, \sigma_{2^n-1}]$ be defined as in (3.7). We then have

$$(3.16) \quad h_{2^n-1} = h_0 + \sum_{k=1}^n \left(\left\lfloor \frac{s_k}{2} \right\rfloor + 1 \right) = -2^n + 1 + \sum_{k=1}^n [(2^{k-1} - 1) + 1] = 0,$$

where $s_{2^n-1} = 0$, $\sigma_{2^n-1} = 1$.

Consider the digital line $D^n \langle (k+1)2^n, 2^n - 1 \rangle$. By (3.9), $h' = (k+1)2^n$, $s' = 2^n - 1$,

$$|(R^n)^{-1}[\delta_{h,s}^n](h', s')| = ((k+1)2^n)^n \geq 2^{2n}(k+1)^n \gtrsim k^n.$$

In contrast, $\|\chi_{k-1} \cdot (R^n \chi_k \cdot (R^n)^{-1} - \text{Id})\|_\infty = 0$ for $k \geq 1$, from the fact that all the digital lines that correspond to the points in $\text{supp}(\chi_{k-1} \cdot R^n)$ lie within $\text{supp} \chi_k$.

3.3. Localization Lemma. To characterize the range of the images in $f \in \mathcal{F}_0^n$, we first prove some lemmas. Let us define the set, for each $m = 1, \dots, n$,

$$(3.17) \quad E_{m,\ell}^n := \left\{ (h,s) \in \mathbb{Z} \times I_{2^n} \mid -(s \% 2^m) \leq h \leq 2^n - 1, s - \ell 2^m \in I_{2^m} \right\},$$

and define $E_{0,\ell}^n := I_{2^n} \times \{\ell\}$. We will denote $E^n := E_{n,0}^n$. and let $E_m^n := \bigcup_{\ell \in I_{2^{n-m}}} E_{m,\ell}^n$. A depiction of these sets appear in Figure 3.3.

The following lemma states that if $f \in \mathcal{F}_0^n$ then $\text{supp } R_{m,\ell}^n[f] \subset E_{m,\ell}^n$, so that the support of $R_{m,\ell}^n[f]$ is restricted in a specific manner.

LEMMA 3.5 (Support of $R_m^n[f]$ for $f \in \mathcal{F}_0^n$).

- (i) If $g \in \mathcal{F}^n$ with $\text{supp } g \subset E_{m,2\ell}^n \cup E_{m,2\ell+1}^n$ then $S_m^n[g] \subset E_{m+1,\ell}^n$.
- (ii) If $f \in \mathcal{F}_0^n$, it holds that $\text{supp } R_m^n[f] \subset E_m^n$.

Proof. (i) By the definition of S_m^n ,

$$\begin{aligned} S_m^n[g] &= \sum_{(h,s+(2\ell)2^m) \in E_{m,2\ell}^n} g(h,s) \delta_{h,2s+1+\ell 2^{m+1}}^n \\ &+ \sum_{(h,s+(2\ell+1)2^m) \in E_{m,2\ell+1}^n} g(h+s+1,s) \delta_{h,2s+1+\ell 2^{m+1}}^n \\ &+ \sum_{(h,s+(2\ell)2^m) \in E_{m,2\ell}^n} g(h,s) \delta_{h,2s+\ell 2^{m+1}}^n \\ &+ \sum_{(h+s,s+(2\ell+1)2^m) \in E_{m,2\ell+1}^n} g(h+s,s) \delta_{h,2s+\ell 2^{m+1}}^n. \end{aligned}$$

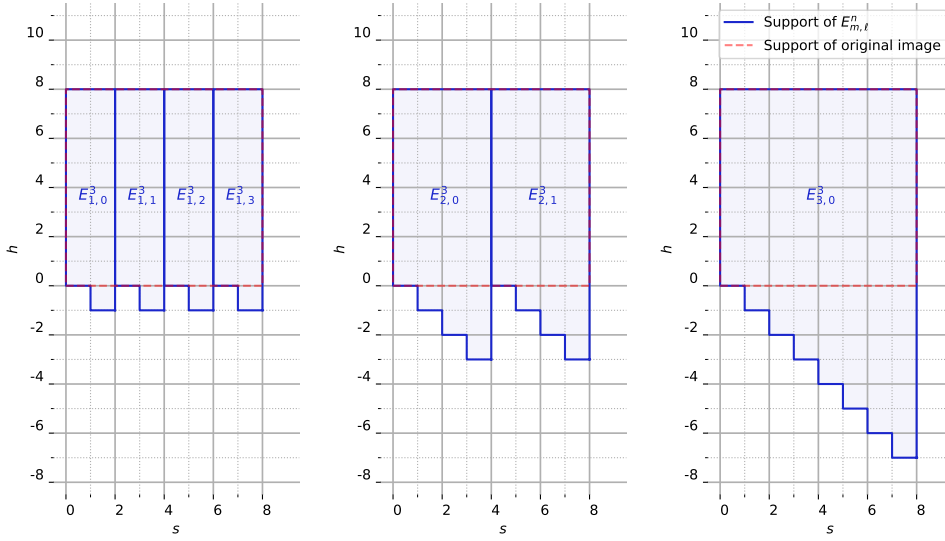


Fig. 3.3: Diagram depicting the set $E_{m,\ell}^n$ (3.17).

Then looking into the first two terms,

$$g_0 := \sum_{s=0}^{2^{m+1}-1} \sum_{h=-s}^{2^n-1} [g(h, s + (2\ell)2^m) + g(h + s, s + (2\ell + 1)2^m)] \delta_{h, 2s+1+\ell 2^m}^n,$$

therefore $\text{supp } g_0 \subset E_{m,\ell}^n$. A similar calculation for the latter two terms which we let g_1 shows that $\text{supp } g_1 \subset E_{m,\ell}^n$.

(ii) Follows from (i), since $R_m^n[f]$ is just repeated compositions of S_m^n . \square

Owing to the two types of sums that describe S_m in (2.7), the map $S_m^n[g]$ for $g \in \mathcal{F}^n$ and $\text{supp } g \in E_m^n$ can also be written as a linear sum of two types of images, which we now describe. Let us define the functions for each $q \in I_{2^{m-1}}$,

$$(3.18) \quad \begin{aligned} \Phi_{m,\ell,q}^n &:= \{\phi_{m,\ell,p,q}^n\}_{p=-2q}^{2^n-1}, & \phi_{m,\ell,p,q}^n &:= \delta_{p, 2q+\ell 2^m}^n + \delta_{p, 2q+1+\ell 2^m}^n. \\ \Psi_{m,\ell,q}^n &:= \{\psi_{m,\ell,p,q}^n\}_{p=-2q}^{2^n-1}, & \psi_{m,\ell,p,q}^n &:= \delta_{p, 2q+\ell 2^m}^n + \delta_{p-1, 2q+1+\ell 2^m}^n. \end{aligned}$$

Then define their collections, for $\ell \in I_{2^{n-m}}$,

$$(3.19) \quad \begin{aligned} \Phi_{m,\ell}^n &:= \bigcup_{q \in I_{2^{m-1}}} \Phi_{m,\ell,q}^n, & \Phi_m^n &:= \bigcup_{\ell \in I_{2^{n-m}}} \Phi_{m,\ell}^n, \\ \Psi_{m,\ell}^n &:= \bigcup_{q \in I_{2^{m-1}}} \Psi_{m,\ell,q}^n, & \Psi_m^n &:= \bigcup_{\ell \in I_{2^{n-m}}} \Psi_{m,\ell}^n. \end{aligned}$$

Then we have $\text{supp } \Phi_{m,\ell}^n, \text{supp } \Psi_{m,\ell}^n \in E_{m,\ell}^n$, where $\text{supp } \Phi := \bigcup_{\phi \in \Phi} \text{supp } \phi$.

LEMMA 3.6 (Linear independence and orthogonal relations).

(i) Φ_m^n and Ψ_m^n are each orthogonal individually.

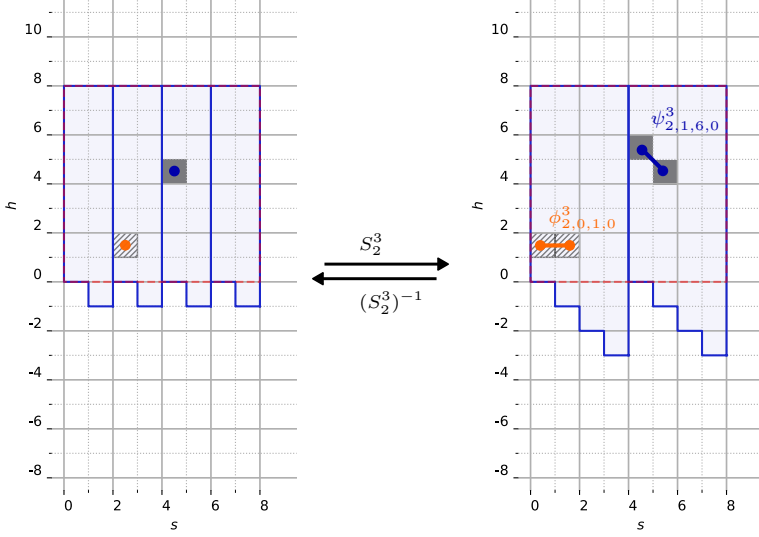


Fig. 3.4: A diagram depicting localization ([Lemma 3.7](#))

- (ii) $\Phi_{m,\ell,q}^n \perp \Psi_{m,\ell,q'}^n$, whenever $q \neq q'$.
- (iii) $\Phi_{m,\ell,q}^n \cup \Psi_{m,\ell,q}^n$ is a linearly independent set.

Proof.

- (i) Whenever $(\ell, p, q) \neq (\ell', p', q')$, we have $\text{supp } \phi_{m,\ell,p,q}^n$ and $\text{supp } \phi_{m,\ell',p',q'}^n$ do not intersect, so that $\phi_{m,\ell,p,q}^n \cdot \phi_{m,\ell',p',q'}^n = 0$. So Φ_m^n is orthogonal, and by the same argument Ψ_m^n is also.
- (ii) Since $\text{supp } \phi_{m,\ell,p,q}^n, \text{supp } \psi_{m,\ell,p,q}^n \subset \mathbb{Z} \times \{2p + \ell 2^m, 2p + 1 + \ell 2^m\}$, it follows that $\text{supp } \phi_{m,\ell,p,q}^n \cap \text{supp } \psi_{m,\ell',p',q'}^n = \emptyset$ whenever $q \neq q'$. So the result follows.
- (iii) Due to (i) and (ii), it only remains to show that $\Phi_{m,\ell}^n \cup \Psi_{m,\ell}^n$ form a linearly independent set. Let $J = 2(2^n + (2q \% 2^{m-1}))$. We form the real matrix $\mathbf{A} \in \mathbb{R}^{J \times J}$ with entries given by

$$(3.20) \quad \mathbf{A}_{i,j} = \xi_i \cdot \xi_j, \quad i, j \in I_J, \quad \text{where} \quad \begin{cases} \xi_{2j} = \phi_{m,\ell,p,j}^n, \\ \xi_{2j+1} = \psi_{m,\ell,p,j}^n, \end{cases} \quad j \in I_{J/2}.$$

It is straightforward to see that $\mathbf{A}_{i,j} = 2$ when $i = j$, and $\mathbf{A}_{i,j} = 1$ when $|i - j| = 1$. So \mathbf{A} is diagonally dominant and therefore non-singular, showing that $\{\xi_j\}_{j=1}^J = \Phi_{m,\ell,q}^n \cup \Psi_{m,\ell,q}^n$ is linearly independent. \square

We will soon see that some of the images in $\Phi_{m,\ell}^n$, $\Psi_{m,\ell}^n$ are not necessary to express $S_m^n[g]$ for $g \in \mathcal{F}^n$ with $\text{supp } g \subset E_{m-1}^n$. To this end, let us partition $\Phi_{m,\ell,q}^n$

and $\Psi_{m,\ell,q}^n$ each into two sets. For $q \in I_{2^m-1}$,

$$(3.21) \quad \begin{aligned} \bar{\Phi}_{m,\ell,q}^n &:= \{\phi_{m,\ell,p,q}^n\}_{p=-q}^{2^n-1}, & \bar{\Psi}_{m,\ell,q}^n &:= \{\psi_{m,\ell,p,q}^n\}_{p=-2q}^{2^n-q-1}, \\ \underline{\Phi}_{m,\ell,q}^n &:= \{\phi_{m,\ell,p,q}^n\}_{p=-2q}^{-q-1}, & \underline{\Psi}_{m,\ell,q}^n &:= \{\psi_{m,\ell,p,q}^n\}_{p=2^n-q}^{2^n}. \end{aligned}$$

An illustration of the members in $\bar{\Phi}_m^n$ and $\bar{\Psi}_m^n$ are shown in [Figure 3.5](#).

Similarly as before, we let

$$(3.22) \quad \begin{aligned} \bar{\Phi}_{m,\ell}^n &:= \bigcup_{q \in I_{2^m-1}} \bar{\Phi}_{m,\ell,q}^n, & \bar{\Psi}_{m,\ell}^n &:= \bigcup_{q \in I_{2^m-1}} \bar{\Psi}_{m,\ell,q}^n, \\ \underline{\Phi}_{m,\ell}^n &:= \bigcup_{q \in I_{2^m-1}} \underline{\Phi}_{m,\ell,q}^n, & \underline{\Psi}_{m,\ell}^n &:= \bigcup_{q \in I_{2^m-1}} \underline{\Psi}_{m,\ell,q}^n, \\ \bar{\Phi}_m^n &:= \bigcup_{\ell \in I_{2^m-1}} \bar{\Phi}_{m,\ell}^n, & \bar{\Psi}_m^n &:= \bigcup_{\ell \in I_{2^m-1}} \bar{\Psi}_{m,\ell}^n, \\ \underline{\Phi}_m^n &:= \bigcup_{\ell \in I_{2^m-1}} \underline{\Phi}_{m,\ell}^n, & \underline{\Psi}_m^n &:= \bigcup_{\ell \in I_{2^m-1}} \underline{\Psi}_{m,\ell}^n. \end{aligned}$$

Let $\bar{\Phi}^n := \bar{\Phi}_n^n, \bar{\Psi}^n := \bar{\Psi}_n^n, \underline{\Phi}^n := \underline{\Phi}_n^n, \underline{\Psi}^n := \underline{\Psi}_n^n$ as well.

For an image $g \in \mathcal{F}^n$, if $S_m^n[g]$ belongs to $\text{span}(\bar{\Phi}_{m,\ell}^n \cup \bar{\Psi}_{m,\ell}^n)$, one can deduce whether the support of f overlaps with $E_{m,2\ell}^n$ or $E_{m,2\ell+1}^n$ by writing $S_m^n[g]$ as a linear sum of members of $\bar{\Phi}_{m,\ell}^n \cup \bar{\Psi}_{m,\ell}^n$ and checking if the coefficients corresponding to those of $\bar{\Phi}_{m,\ell}^n$ or $\bar{\Psi}_{m,\ell}^n$ vanish.

LEMMA 3.7 (Localization). *Let $g = S_m^n[g_0 + g_1]$ where $g_0, g_1 \in \mathcal{F}^n$, $\text{supp } g_0 \in E_{m-1,2\ell}^n, \text{supp } g_1 \in E_{m-1,2\ell+1}^n$ then $g \in \text{span}(\bar{\Phi}_{m,\ell}^n \cup \bar{\Psi}_{m,\ell}^n)$. And furthermore,*

- (i) if $g \in \text{span } \bar{\Phi}_{m,\ell}^n$ then $g_1 = 0$,
- (ii) if $g \in \text{span } \bar{\Psi}_{m,\ell}^n$ then $g_0 = 0$.

Proof. Let us write,

$$(3.23) \quad g_0 = \sum_{(h,s) \in E^m} g_0(h,s) \delta_{h,s}^n, \quad g_1 = \sum_{(h,s) \in E^m} g_1(h,s) \delta_{h,s}^n.$$

Then by (2.7), we have

$$\begin{aligned}
(3.24) \quad g &= \sum_{(h,s) \in E_{m,2\ell}^n} g_0(h,s) \delta_{h,2s+1}^n + \sum_{(h+s+1,s) \in E_{m,2\ell+1}^n} g_1(h+s+1,s) \delta_{h,2s+1}^n \\
&\quad + \sum_{(h,s) \in E_{m,2\ell}^n} g_0(h,s) \delta_{h,2s}^n + \sum_{(h+s,s) \in E_{m,2\ell+1}^n} g_1(h+s,s) \delta_{h,2s}^n \\
&= \sum_{(h,s) \in E_{m,2\ell}^n} g_0(h,s) (\delta_{h,2s}^n + \delta_{h,2s+1}^n) \\
&\quad + \sum_{(h,s) \in E_{m,2\ell+1}^n} g_1(h,s) (\delta_{h-s,2s}^n + \delta_{h-s-1,2s+1}^n) \\
&= \sum_{s=0}^{2^m-1} \sum_{h=-s}^{2^n-1} g_0(h,s) (\delta_{h,2s}^n + \delta_{h,2s+1}^n) \\
&\quad + \sum_{s=0}^{2^m-1} \sum_{h=-s}^{2^n-1} g_1(h,s) (\delta_{h-s,2s}^n + \delta_{h-s-1,2s+1}^n),
\end{aligned}$$

then using the definitions of the basis ψ and ϕ (3.18),

$$(3.25) \quad g = \sum_{q=0}^{2^m-1} \sum_{p=-q}^{2^n-1} g_0(p,q) \phi_{m,\ell,p,q}^n + \sum_{q=0}^{2^m-1} \sum_{p=-q}^{2^n-1} g_1(p,q) \psi_{m,\ell,p-q,q}^n.$$

Rearranging, we arrive at

$$(3.26) \quad g = \sum_{q=0}^{2^m-1} \sum_{p=-q}^{2^n-1} g_0(p,q) \phi_{m,\ell,p,q}^n + \sum_{q=0}^{2^m-1} \sum_{p=-2q}^{2^n-q-1} g_1(p,q) \psi_{m,\ell,p,q}^n,$$

showing that $g \in \text{span}(\bar{\Phi}_{m,\ell}^n \cup \bar{\Psi}_{m,\ell}^n)$. Recall that the set $\bar{\Phi}_{m,\ell}^n \cup \bar{\Psi}_{m,\ell}^n$ is linearly independent, so the expansion (3.26) is unique. Hence, if $f \in \text{span} \bar{\Phi}_{m,\ell}^n$ it must be that $f_0 = 0$. Similarly, if $f \in \text{span} \bar{\Psi}_{m,\ell}^n$ then $f_1 = 0$. \square

Note that the inversion formula (2.29) is a backward substitution formula applied to the linear system (3.26).

Now, we turn our attention to the space of images $f \in \mathcal{F}^n$ whose support lies in $E_{m,\ell}^n$ defined for $m \in I_{n+1}$

$$(3.27) \quad \mathcal{G}_{m,\ell}^n := \{f \in \mathcal{F}^n : \text{supp } f \in E_{m,\ell}^n\}, \quad \mathcal{G}_m^n := \bigcup_{\ell \in I_{2^n-m}} \mathcal{G}_{m,\ell}^n.$$

Above, we have shown $g \in \mathcal{G}_{m,\ell}^n$ such that $g = S_m^n[g_0 + g_1]$ for some $g_0 \in \mathcal{G}_{m-1,2\ell}^n$, $g_1 \in \mathcal{G}_{m-1,2\ell+1}^n$ to belong to $\text{span}(\bar{\Phi}_{m,\ell}^n \cup \bar{\Psi}_{m,\ell}^n)$, and therefore to $\text{span}(\Phi_{m,\ell}^n \cup \Psi_{m,\ell}^n)$. Then, it is natural to ask which of those $f \in \mathcal{G}_{m,\ell}^n$ do *not* belong to $\text{span}(\Phi_{m,\ell}^n \cup \Psi_{m,\ell}^n)$? We answer this question next.

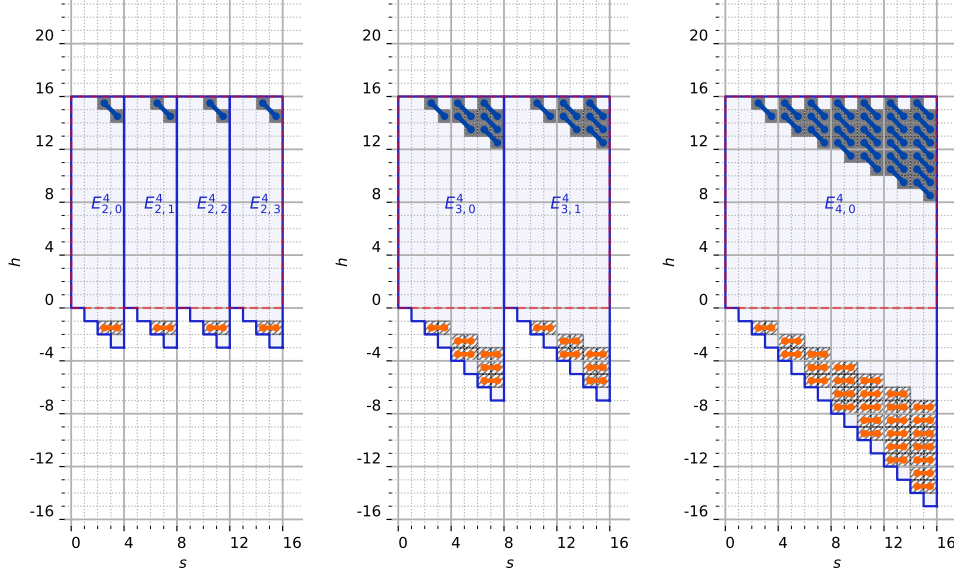


Fig. 3.5: An illustration of members of Φ_m^n and Ψ_m^n for $n = 4$ with $m = 2$ (left), $m = 3$ (middle) and $m = 4$ (right).

Let us define $\mu_{m,\ell,q}^n \in \mathcal{F}^n$ given by

$$\begin{aligned}
 (3.28) \quad \mu_{m,\ell,q}^n(h, s) &= \begin{cases} 1 & \text{if } -2q \leq h \leq 2^n - 1 \text{ and } s = 2q + \ell 2^m. \\ -1 & \text{if } -2q - 1 \leq h \leq 2^n - 1 \text{ and } s = 2q + 1 + \ell 2^m, \\ 0 & \text{otherwise.} \end{cases} \\
 &= \sum_{p=-2q}^{2^n-1} \delta_{p,2q+\ell 2^m}^n(h, s) - \sum_{p=-2q-1}^{2^n-1} \delta_{p,2q+1+\ell 2^m}^n
 \end{aligned}$$

and correspondingly let

$$(3.29) \quad M_{m,\ell}^n := \{\mu_{m,\ell,q}^n\}_{q \in I_{2^m-1}}.$$

Note that $M_{m,\ell}^n$ forms an orthogonal set, as $\text{supp } \mu_{m,\ell,q}^n \cap \text{supp } \mu_{m,\ell,q'}^n = \emptyset$ for $q \neq q'$.

LEMMA 3.8 (Mass constraints). *Suppose $g \in \mathcal{G}_{m,\ell}^n$, then $g \in \text{span}(\Phi_{m,\ell}^n \cup \Psi_{m,\ell}^n)$ if and only if $g \cdot \mu = 0$ for all $\mu \in M_{m,\ell}^n$. Equivalently,*

$$(3.30) \quad \sum_{h=-2t}^{2^n-1} g(h, 2t + \ell 2^m) = \sum_{h=-2t-1}^{2^n-1} g(h, 2t + 1 + \ell 2^m) \quad \text{for } t \in I_{2^{m-1}}.$$

Proof. The members of $\Phi_{m,\ell}^n$ and $\Psi_{m,\ell}^n$ themselves satisfy this constraint: for $q \in I_{2^{m-1}}$

$$\begin{aligned} \sum_{h=-2t}^{2^n} \phi_{m,\ell,p,q}^n(h, 2t) &= \sum_{h=-2t-1}^{2^n} \phi_{m,\ell,p,q}^n(h, 2t + 1), \\ \sum_{h=-2t}^{2^n} \psi_{m,\ell,p,q}^n(h, 2t) &= \sum_{h=-2t-1}^{2^n} \psi_{m,\ell,p,q}^n(h, 2t + 1). \end{aligned}$$

That is, $\mu \cdot \psi = 0$ for all $\mu \in M_{m,\ell}^n$ and $\psi \in \Phi_{m,\ell}^n \cup \Psi_{m,\ell}^n$. So if $g \in \text{span}(\Phi_{m,\ell}^n \cup \Psi_{m,\ell}^n)$ then $g \cdot \mu = 0$.

Conversely, $E_{m,\ell,q}^n = E_{m,\ell}^n \cap (\mathbb{Z} \times \{2q, 2q + 1\})$ ($q \in I_{2^{m-1}}$) has $2 \cdot 2^n + 4q + 1$ members, whereas $|\Phi_{m,\ell,q}^n| + |\Psi_{m,\ell,q}^n| = (2^n + 2q) + (2^n + 2q) = 2 \cdot 2^n + 4q$. As noted above, $\mu_{m,\ell,p,q}^n \cdot \psi = 0$ for all $\psi \in \Phi_{m,\ell,q}^n \cup \Psi_{m,\ell,q}^n$. Hence $\{\mu_{m,\ell,p,q}^n\} \cup \Phi_{m,\ell,q}^n \cup \Psi_{m,\ell,q}^n$ form a basis for functions in \mathcal{F}^n supported in $E_{m,\ell,q}^n$. Therefore $g \cdot \mu_{m,\ell,p,q}^n = 0$ implies $g \in \text{span}(\Phi_{m,\ell,q}^n \cup \Psi_{m,\ell,q}^n)$ for all $q \in I_{2^{m-1}}$, implying that $g \in \text{span}(\Phi_{m,\ell}^n \cup \Psi_{m,\ell}^n)$. \square

The constraint (3.30) is interpreted as a sort of a mass consistency condition. If $g = R_{m,\ell}^n[f]$ for some $f \in \mathcal{F}_0^n$, then the constraint implies that

$$(3.31) \quad \sum_{h=-2t}^{2^n-1} R_{m,\ell}^n[f](h, 2t) = \sum_{h=-2t-1}^{2^n-1} R_{m,\ell}^n[f](h, 2t + 1).$$

This condition is always satisfied for such g since the sum of f over digital lines of different slopes $2t$ and $2t + 1$,

$$\bigcup_{h=-2t}^{2^n-1} D_{m,\ell}^n \langle h, 2t \rangle, \quad \text{and} \quad \bigcup_{h=-2t-1}^{2^n-1} D_{m,\ell}^n \langle h, 2t + 1 \rangle,$$

must both equal the total sum $\sum_{(i,j) \in \mathbb{Z} \times I_{2^m}} f_{m,\ell}^n(i, j)$ of all values of f .

3.4. Characterization of $R^n[\mathcal{F}_0^n]$. Now we characterize the range of \mathcal{F}_0^n under R^n . First, note that the range of S_m^n is straightforward to characterize, due to the lemmas from the preceding section.

First, it follows from Lemma 3.6 and Lemma 3.8 that

$$(3.32) \quad \mathcal{G}_{m,\ell}^n = \text{span}(\overline{\Phi}_{m,\ell}^n \cup \overline{\Psi}_{m,\ell}^n \cup \underline{\Phi}_{m,\ell}^n \cup \underline{\Psi}_{m,\ell}^n \cup M_{m,\ell}^n),$$

in which $\overline{\Phi}_{m,\ell}^n, \overline{\Psi}_{m,\ell}^n, \underline{\Phi}_{m,\ell}^n, \underline{\Psi}_{m,\ell}^n$ defined in (3.21), and $M_{m,\ell}^n$ in (3.29).

We will separate $\mathcal{G}_{m,\ell}^n$ in two, by writing

$$(3.33) \quad \mathcal{G}_{m,\ell}^n = \text{span } X_{m,\ell}^n \oplus \text{span } Y_{m,\ell}^n,$$

where \oplus denotes the direct sum and

$$(3.34) \quad X_{m,\ell}^n := \overline{\Phi}_{m,\ell}^n \cup \overline{\Psi}_{m,\ell}^n, \quad Y_{m,\ell}^n := \underline{\Phi}_{m,\ell}^n \cup \underline{\Psi}_{m,\ell}^n \cup M_{m,\ell}^n.$$

We will also let,

$$X_m^n := \bigcup_{\ell \in I_{2^n-m}} X_{m,\ell}^n, \quad Y_m^n := \bigcup_{\ell \in I_{2^n-m}} Y_{m,\ell}^n.$$

Let $P_{m,\ell}^n$ be a projection to $\text{span } Y_{m,\ell}^n$, and P_m^n a projection to $\text{span } Y_m^n$.

LEMMA 3.9. *It holds that $S_m^n[\mathcal{G}_{m-1}^n] = \text{span } X_m^n$ for $m = 1, \dots, n$.*

Proof. Let $g = S_m^n[f]$ for some $f \in \mathcal{G}_{m-1}^n$, then $g \in \text{span } X_m^n$ by Lemma 3.7, so $S_m^n[\mathcal{G}_{m-1}^n] \subset \text{span } X_m^n$. Conversely, if $g \in \text{span } X_m^n$ then $(S_m^n)^{-1}[g] \in \mathcal{G}_{m-1}^n$ by Lemma 3.7, so $S_m^n[\mathcal{G}_{m-1}^n] \supset \text{span } X_m^n$. \square

We will now characterize the range $R^n[\mathcal{F}_0^n]$. So far, we know from Lemma 3.5 that R^n maps \mathcal{F}_0^n into \mathcal{G}^n (3.27), and have shown in Theorem 3.3 that $R^n : \mathcal{F}_+^n \rightarrow \mathcal{F}_+^n$ is a bijection by the virtue of the inversion formula (2.30). Then we showed that $S_m^n[\mathcal{G}_m^n] = \text{span } X_m^n$ in Lemma 3.9. These facts will enable us to characterize $R^n[\mathcal{F}_0^n] \subset \mathcal{G}^n$ with a set of linear constraints.

We define the partial inverse $T_m^n : \mathcal{F}_+^n \rightarrow \mathcal{F}_+^n$ as given by

$$(3.35) \quad \begin{cases} T_m^n := (S_{m+1}^n)^{-1} \circ \dots \circ (S_n^n)^{-1} \text{ for } m = 2, \dots, n-1, \\ T_n^n := \text{Id}. \end{cases}$$

Now, we will define the space of images formed from $g \in \mathcal{G}^n$ (3.27) for which $T_m^n[g]$ has projection P_m^n to $\text{span } Y_m^n$ (3.33) is zero.

$$(3.36) \quad \mathcal{F}_R^n = \{g \in \mathcal{G}^n \mid P_m^n \circ T_m^n[g] = 0, \ m = 2, \dots, n\}.$$

We will show that \mathcal{F}_R^n is the range of \mathcal{F}_0^n under R^n .

THEOREM 3.10 (Range characterization of R^n). *$R^n : \mathcal{F}_0^n \rightarrow \mathcal{F}_R^n$ is a bijection.*

Proof. For $f \in \mathcal{F}_0^n$, $\text{supp } f \subset I_{2^n} \times I_{2^n}$ so f can be identified to a function from $I_{2^n} \times I_{2^n}$ to \mathbb{R} , hence f has $|I_{2^n} \times I_{2^n}| = 2^{2n} = N^2$ degrees of freedom, and $R^n[f] \subset \mathcal{G}^n$. Any $g \in \mathcal{G}^n$ is identified to an image from E^n to \mathbb{R} , so the number of degree of freedoms for g is

$$|E^n| = 2^{2n} + 2^{2n-1} - 2^{n-1} = N^2 + \frac{N(N-1)}{2} = \frac{3}{2}N^2 - \frac{1}{2}N.$$

To show that $R^n : \mathcal{F}_0^n \rightarrow \mathcal{F}_R^n$ is a bijection, it suffices to show that the constraints

$$(3.37) \quad P_m^n \circ T_m^n[g] = 0 \quad \text{for } m = 2, \dots, n,$$

form $N(N-1)/2$ linearly independent constraints.

Now, consider the identity

$$(3.38) \quad \begin{aligned} (S_m^n)^{-1}[\mathcal{G}_m^n] &= (S_m^n)^{-1}[\text{span } X_m^n] \oplus (S_m^n)^{-1}[\text{span } Y_m^n] \\ &= \mathcal{G}_{m-1}^n \oplus (S_m^n)^{-1}[\text{span } Y_m^n]. \end{aligned}$$

Applying this to \mathcal{G}^n ,

$$(3.39) \quad \begin{aligned} (R^n)^{-1}[\mathcal{G}^n] &= (S_1^n)^{-1} \circ \dots \circ (S_n^n)^{-1}[\mathcal{G}^n] \\ &= (S_1^n)^{-1} \circ \dots \circ (S_n^n)^{-1}[\text{span } X^n \oplus \text{span } Y^n] \\ &= (S_1^n)^{-1} \circ \dots \circ (S_{n-1}^n)^{-1}[\mathcal{G}_{n-1}^n \oplus (S_n^n)^{-1}[\text{span } Y^n]]. \end{aligned}$$

Then repeating,

$$(3.40) \quad \begin{aligned} &(S_1^n)^{-1} \circ \dots \circ (S_{n-1}^n)^{-1}[\mathcal{G}_{n-1}^n \oplus (S_n^n)^{-1}[\text{span } Y^n]] \\ &= (S_1^n)^{-1} \circ \dots \circ (S_{n-1}^n)^{-1}[\text{span } X_{n-1}^n \oplus \text{span } Y_{n-1}^n \oplus (S_n^n)^{-1}[\text{span } Y^n]] \\ &= ((S_1^n)^{-1} \circ \dots \circ (S_{n-2}^n)^{-1}) \\ &\quad [\mathcal{G}_{n-2}^n \oplus (S_{n-1}^n)^{-1}[\text{span } Y_{n-1}^n] \oplus (S_{n-1}^n)^{-1} \circ (S_n^n)^{-1}[\text{span } Y^n]] \\ &= \dots = \mathcal{G}_0^n \oplus \left(\bigoplus_{m=1}^n (R_m^n)^{-1}[\text{span } Y_m^n] \right). \end{aligned}$$

Note that since R_m^n is a bijection from $\mathbb{Z} \times I_{2^n}$ to $\mathbb{Z} \times I_{2^n}$, for $g \in \mathcal{G}^n$, we have that $P_{m,\ell}^n \circ T_m^n[g] = 0$ if and only if $P_m^n \circ R_m^n \circ (R_m^n)^{-1} \circ T_m^n[g] = 0$, and writing $Q_m^n := P_m^n \circ R_m^n$, $Q_{m,\ell}^n$ is a projection in \mathcal{F}^n to the subspace

$$\text{span } Z_m^n \quad \text{where } Z_m^n := (R_m^n)^{-1}[Y_m^n].$$

Thus, the constraint $P_m^n \circ T_m^n[g] = 0$ is equivalent to $Q_m^n \circ (R^n)^{-1}[g] = 0$. Now, since $\mathcal{G}_0^n = \mathcal{F}_0^n$,

$$(3.41) \quad (R^n)^{-1}[\mathcal{G}^n] = \mathcal{F}_0^n \oplus \left(\bigoplus_{m=1}^n \text{span } Z_m^n \right),$$

and the projection Q_m^n is linearly independent spaces $\text{span } Z_m^n$, and the set of constraints $P_m^n \circ T_m^n[g] = 0$ for $m = 2, \dots, n$ are linearly independent.

We next count the number of constraints. The total number $\mathcal{C}(N)$ of constraints is composed of the mass constraints $\mathcal{C}_M(N)$ and the support constraints $\mathcal{C}_S(N)$, $\mathcal{C}(N) = \mathcal{C}_M(N) + \mathcal{C}_S(N)$. Then, we have $N/2$ mass constraints at each application of S_m^n (2.7)

for $m = 1, \dots, n$ is $C_M(N) = \frac{N}{2}n$. The number of additional constraints given by the projections P_m^n at each $m = 2, \dots, n$ is given by

$$(3.42) \quad |\underline{\Phi}_m^n| + |\underline{\Psi}_m^n| = 2^{m-1} \cdot (2^{m-1} - 1) \cdot 2^{n-m} = N \frac{2^{m-1} - 1}{2}.$$

Note that when $m = 1$ there are no constraints, as $\underline{\Phi}_1^n, \underline{\Psi}_1^n = \emptyset$: as $|E_1^n| = N^2 + N/2$ for $\ell \in I_{2^{n-1}}$ with $N/2$ extra degrees of freedom, which matches the number of mass constraints for $m = 1$.

So the total number of constraints is

$$(3.43) \quad \begin{aligned} C(N) &= \frac{N}{2}n + N \left(\sum_{m=2}^n \frac{2^{m-1} - 1}{2} \right) \\ &= \frac{N}{2}n + N \left(\sum_{m=2}^n 2^{m-2} \right) - N \left(\sum_{m=2}^n \frac{1}{2} \right) = \frac{N(N-1)}{2}. \end{aligned}$$

The number of linearly independent constraints match the redundant number of degrees of freedom, proving the claim. \square

Acknowledgements. WL was supported by AMS Simons Travel grant. The work of KR is partially supported by the National Science Foundation through grants DMS-1913309 and DMS-1937254. The work of DR was partially supported by the Air Force Center of Excellence on Multi-Fidelity Modeling of Rocket Combustor Dynamics under Award Number FA9550-17-1-0195 and AFOSR MURI on multi-information sources of multi-physics systems under Award Number FA9550-15-1-0038.

REFERENCES

- [1] A. AVERBUCH, R. R. COIFMAN, D. L. DONOHO, M. ISRAELI, AND Y. SHKOLNISKY, *A framework for discrete integral transformations I—the pseudopolar fourier transform*, SIAM Journal on Scientific Computing, 30 (2008), pp. 764–784.
- [2] A. AVERBUCH, R. R. COIFMAN, D. L. DONOHO, M. ISRAELI, Y. SHKOLNISKY, AND I. SEDELNIKOV, *A framework for discrete integral transformations II—the 2D discrete Radon transform*, SIAM Journal on Scientific Computing, 30 (2008), pp. 785–803.
- [3] G. BEYLKIN, *Discrete radon transform*, IEEE Transactions on Acoustics, Speech, and Signal Processing, 35 (1987), pp. 162–172.
- [4] N. BONNEEL, J. RABIN, G. PEYRÉ, AND H. PFISTER, *Sliced and Radon Wasserstein barycenters of measures*, Journal of Mathematical Imaging and Vision, 51 (2015), pp. 22–45.
- [5] M. L. BRADY, *A fast discrete approximation algorithm for the Radon transform*, SIAM Journal on Computing, 27 (1998), pp. 107–119.
- [6] A. M. CORMACK, *Representation of a Function by Its Line Integrals, with Some Radiological Applications*, Journal of Applied Physics, 34 (1963), pp. 2722–2727.
- [7] S. R. DEANS, *The Radon Transform and Some of Its Applications*, Wiley, 1983.
- [8] J. FRANK, *Three-Dimensional Electron Microscopy of Macromolecular Assemblies*, Academic Press, Burlington, 1996.
- [9] W. GÖTZ AND H. DRUCKMÜLLER, *A fast digital radon transform: an efficient means for evaluating the hough transform*, Pattern Recognition, 29 (1996), pp. 711 – 718.

- [10] S. HELGASON, *The Radon Transform*, Springer, Boston, MA., 1999.
- [11] J. ILMAVIRTA, *On Radon transforms on tori*, Journal of Fourier Analysis and Applications, 21 (2015), pp. 370–382.
- [12] J. ILMAVIRTA, O. KOSKELA, AND J. RAILO, *Torus computed tomography*, SIAM Journal on Applied Mathematics, 80 (2020), pp. 1947–1976.
- [13] J. ILMAVIRTA AND F. MONARD, *4. Integral geometry on manifolds with boundary and applications*, De Gruyter, 2019, pp. 43–114.
- [14] J. ILMAVIRTA AND G. UHLMANN, *Tensor tomography in periodic slabs*, Journal of Functional Analysis, 275 (2018), pp. 288–299.
- [15] S. G. KAZANTSEV AND A. A. BUKHGEIM, *Singular value decomposition for the 2d fan-beam radon transform of tensor fields*, Journal of Inverse and Ill-Posed Problems, 12 (2004), pp. 245–278.
- [16] B. T. KELLEY AND V. K. MADISETTI, *The fast discrete Radon transform. I. Theory*, IEEE Transactions on Image Processing, 2 (1993), pp. 382–400.
- [17] P. D. LAX AND R. S. PHILLIPS, *Scattering theory*, Bull. Amer. Math. Soc., 70 (1964), pp. 130–142.
- [18] A. K. LOUIS, *Orthogonal Function Series Expansions and the Null Space of the Radon Transform*, SIAM Journal on Mathematical Analysis, 15 (1984), pp. 621–633.
- [19] A. K. LOUIS, *Tikhonov-Phillips Regularization of the Radon Transform*, in International Series of Numerical Mathematics, vol 73, G. Hämmerlin and K. H. KH, eds., Birkhäuser, Basel, 1985, ch. International Series of Numerical Mathematics, vol 73.
- [20] A. K. LOUIS AND A. RIEDER, *Incomplete Data Problems in X-Ray Computerized Tomography*, Numer. Math., 56 (1989), pp. 371–383.
- [21] A. K. LOUIS AND T. SCHUSTER, *A novel filter design technique in 2D computerized tomography*, Inverse Problems, 12 (1996), pp. 685–696.
- [22] P. MAASS, *The x-ray transform: singular value decomposition and resolution*, Inverse Problems, 3 (1987), pp. 729–741.
- [23] P. MAASS, *The Interior Radon Transform*, SIAM Journal on Applied Mathematics, 52 (1992), pp. 710–724.
- [24] R. B. MARR, *On the reconstruction of a function on a circular domain from a sampling of its line integrals*, Journal of Mathematical Analysis and Applications, 45 (1974), pp. 357–374.
- [25] F. MATUS AND J. FLUSSER, *Image representation via a finite Radon transform*, IEEE Transactions on Pattern Analysis and Machine Intelligence, 15 (1993), pp. 996–1006.
- [26] P. MIDGLEY AND M. WEYLAND, *3D electron microscopy in the physical sciences: the development of Z-contrast and EFTEM tomography*, Ultramicroscopy, 96 (2003), pp. 413–431. Proceedings of the International Workshop on Strategies and Advances in Atomic Level Spectroscopy and Analysis.
- [27] F. NATTERER, *The Mathematics of Computerized Tomography*, Society for Industrial and Applied Mathematics, 2001.
- [28] W. H. PRESS, *Discrete Radon transform has an exact, fast inverse and generalizes to operations other than sums along lines*, Proceedings of the National Academy of Sciences, 103 (2006), pp. 19249–19254.
- [29] W. H. PRESS, S. A. TEUKOLSKY, W. T. VETTERLING, AND B. P. FLANNERY, *Numerical Recipes in C (2nd Ed.): The Art of Scientific Computing*, Cambridge University Press, USA, 1992.
- [30] E. T. QUINTO, *Singular value decompositions and inversion methods for the exterior radon transform and a spherical transform*, Journal of Mathematical Analysis and Applications, 95 (1983), pp. 437–448.
- [31] J. RADON, *On the determination of functions from their integral values along certain manifolds*, IEEE Transactions on Medical Imaging, 5 (1986), pp. 170–176.
- [32] J. RAILO, *Fourier Analysis of Periodic Radon Transforms*, Journal of Fourier Analysis and Applications, 26 (2020), p. 64.

- [33] D. RIM, *Dimensional Splitting of Hyperbolic Partial Differential Equations Using the Radon Transform*, SIAM Journal on Scientific Computing, 40 (2018), pp. A4184–A4207.
- [34] D. RIM, *Exact and fast inversion of the approximate discrete Radon transform from partial data*, Applied Mathematics Letters, 102 (2020), p. 106159.
- [35] D. RIM AND K. MANDLI, *Displacement Interpolation Using Monotone Rearrangement*, SIAM/ASA Journal on Uncertainty Quantification, 6 (2018), pp. 1503–1531.
- [36] TAI-CHIU HSUNG, D. P. K. LUN, AND WAN-CHI SIU, *The discrete periodic Radon transform*, IEEE Transactions on Signal Processing, 44 (1996), pp. 2651–2657.